Nucl Eng Technol 47 (2015) 875–883

Available online at www.sciencedirect.com

ScienceDirect

journal homepage: http://www.journals.elsevier.com/nuclear-engineering-and-technology/

Original Article

COMPUTATIONAL INVESTIGATION OF ^{99}Mo, ^{89}Sr, AND ^{131}I PRODUCTION RATES IN A SUBCRITICAL $UO_2(NO_3)_2$ AQUEOUS SOLUTION REACTOR DRIVEN BY A 30-MEV PROTON ACCELERATOR

Z. GHOLAMZADEH [a,*], *S.A.H. FEGHHI* [b], *S.M. MIRVAKILI* [a], *A. JOZE-VAZIRI* [a], *and M. ALIZADEH* [a]

[a] *Reactor Research School, Nuclear Science and Technology Research Institute, Kargar, Tehran 0098, Iran*

[b] *Department of Radiation Application, Shahid Beheshti University, G.C., Velenjak, Tehran 0098, Iran*

ARTICLE INFO

Article history:
Received 6 April 2015
Received in revised form
4 August 2015
Accepted 5 August 2015
Available online 21 October 2015

Keywords:
Computational Simulation
Proton Accelerator
Subcritical Aqueous Reactor
Uranyl Nitrate

ABSTRACT

The use of subcritical aqueous homogenous reactors driven by accelerators presents an attractive alternative for producing ^{99}Mo. In this method, the medical isotope production system itself is used to extract ^{99}Mo or other radioisotopes so that there is no need to irradiate common targets. In addition, it can operate at much lower power compared to a traditional reactor to produce the same amount of ^{99}Mo by irradiating targets. In this study, the neutronic performance and ^{99}Mo, ^{89}Sr, and ^{131}I production capacity of a subcritical aqueous homogenous reactor fueled with low-enriched uranyl nitrate was evaluated using the MCNPX code. A proton accelerator with a maximum 30-MeV accelerating power was used to run the subcritical core. The computational results indicate a good potential for the modeled system to produce the radioisotopes under completely safe conditions because of the high negative reactivity coefficients of the modeled core. The results show that application of an optimized beam window material can increase the fission power of the aqueous nitrate fuel up to 80%. This accelerator-based procedure using low enriched uranium nitrate fuel to produce radioisotopes presents a potentially competitive alternative in comparison with the reactor-based or other accelerator-based methods. This system produces ~1,500 Ci/wk (~325 6-day Ci) of ^{99}Mo at the end of a cycle.

1. Introduction

The homogeneous reactor was one of the first reactors built after the first nuclear reactor called Chicago Pile-1. The first reactor of this type was constructed at the end of 1943, running on a uranyl sulfate solution containing 14% enriched uranium. In 1944, the LOPO (low power) reactor went critical using a uranyl sulfate solution of 565 g ^{235}U dissolved in 13 L

* *Corresponding author.*
E-mail address: cadmium_109@yahoo.com (Z. Gholamzadeh).

http://dx.doi.org/10.1016/j.net.2015.08.004
1738-5733/Copyright © 2015, Published by Elsevier Korea LLC on behalf of Korean Nuclear Society.

light water in a sphere with a diameter of 30 cm. Between 1940 and 1980, many aqueous homogenous reactors (AHRs) were built and operated, including SUPO (super power), HYPO (high power), HRE (homogenous reactor experiment), ARGUS, and SILENE reactors [1,2].

Currently, these aqueous reactors are strongly considered for the production of radioisotopes, especially ^{99}Mo. Some countries are developing such AHRs, whereas the design of the subcritical accelerator-driven type is under serious study by other countries [3–5]. In 1995, Ion Beam Applications (IBA, Ottignies-Louvain-la-Neuve, Belgium) Company started to think about new ways to produce ^{99}Mo based on accelerators instead of nuclear reactors [4].

The recovery of molybdenum from a sulfate solution by anion exchange is not as efficient as that from a nitrate or a uranyl nitrate solution, both of which have superior chemical properties relative to uranyl sulfate solutions. However, the radiolytic decomposition of an aqueous uranyl nitrate solution creates nitrogen and nitrogen oxide (NO_x) gases as well as H_2 and O_2, which could make the required off-gas system more complex. By contrast, NO_x release will raise the solution pH. The solubility rates of sulfate salts are generally noticeably lower than those of nitrate salts, and as the fuel ages, the buildup of fission and adsorption products may become high enough to approach solubility limits. The fission products of special concern are Ba, Sr, and rare earth elements [3].

Accelerator-driven subcritical reactors with solid fuels are being designed by several countries. Accelerator-Driven Optimized Nuclear Irradiation System (ADONIS) is one project of this type; it is being run by Belgium and relies on a high-energy high-current cyclotron coupled to a subcritical assembly. The proton beam impinges on a conical spallation target made of tantalum to generate a high-intensity neutron flux. The tantalum target is surrounded by four cylindrical layers of high enriched uranium (HEU) targets interleaved with beryllium moderation rings. The targets have a cylindrical shape with an outer radius of 1.1 cm and a length of 20 cm. They are identical to those used in nuclear reactors. Each target contains 4 g of ^{235}U and is immersed in heavy water (D_2O) for cooling. The subcritical core contains 150 HEU targets surrounded by a thick beryllium reflector [6].

Advanced Medical Isotope Corporation (Okanogan Avenue, Kennewick, USA) licensed a hybrid accelerator-based technology from the University of Missouri to supply a minimum of 50% of the United States' ^{99}Mo needs from a subcritical solution of low enriched uranium (LEU). In this system, an electron beam strikes a high-density tungsten target. The produced photons emerge into a stainless steel tank holding D_2O and LEU salt. The photons eject neutrons from deuterium atoms, initiating fission in the LEU target material, which provides a fission reaction in the LEU target [7].

In this study, investigation of an aqueous subcritical reactor containing uranyl nitrate fuel for producing ^{131}I, ^{89}Sr, and ^{99}Mo radioisotopes was conducted. A CYCLONE 30 proton accelerator was assumed to drive this subcritical core.

AHRs have prominent advantages including: (1) accessibility of high power density because there is virtually no heat-transfer barrier between the fuel and coolant, so reactor power densities of 50–200 kW/L may be possible; (2) unlimited fuel burnup owing to the possibility of continuous removal of poisons as well as continuous addition of new fuel in AHRs; (3) simple fuel preparation and reprocessing; and (4) negative reactivity coefficients. However, AHR systems also have several disadvantages: (1) radiation-induced corrosion; (2) external circulation of fuel solution for extraction of the produced radioisotopes; (3) limited uranium concentration in the fuel solution (<1,000 g/L); and (4) limited operating temperatures [2]. The design of the accelerator-driven aqueous homogenous reactor (ADHR) enhances the aqueous reactor safety owing to the subcritical running of the reactor. Higher burnups are accessible in ADHR systems, and less reprocessing of the solution fuel is required in comparison with commonly used AHRs. Reduction of the effective multiplication of the subcritical nuclear core could conclude in the reduction of output power, but this can be compensated for by beam current enhancement. In addition, the accelerator-driven subcritical aqueous reactors can operate independently of control rods. Therefore, the design and construction of these ADHRs are of interest.

2. Materials and methods

In this study, MCNPX 2.6.0 was used as a powerful particle transport code with the ability to calculate steady-state reaction rates, normalization parameters, neutronic parameters, as well as fuel burnup using CINDER90 to calculate the time-dependent parameters [5,8,9]. A cylindrical aqueous reactor was modeled. Light water flowing inside the considered coils was selected as a coolant for the fuel solution. A three-dimensional neutronic model was set up in cold zero power situations by means of the Evaluated Nuclear Data File (ENDF/B-VI) continuous-energy cross section. The cross sections of S(α, β) were used for the fuel solution, heavy water, and light water. A 25-cm-thick heavy water reflector was considered to reflect the emerging neutrons and perform a controlling role for the system shutdown requirements. The KCODE mode was used for neutronic parameter calculations (Table 1).

The uranium enrichment was 19.75% (^{235}U, 19.75%; ^{238}U, 80.25%) in the nitrate salt. As the following balance equations show, the 0.719M nitrate solution can obtain an approximate pH of 7.5.

$$2UO_2(NO_3)_2 + 2H_2O = 4HNO_3 + 2UO_2 + O_2$$

The fuel solution pH cannot be allowed to rise above 3. If it does, precipitation of uranium and many fission products will begin. To adjust the solution pH, several drops of 13M HNO_3

Table 1 – Core material and dimensions modeled using MCNPX 2.6.0.

Core specifications	Value	Unit
Fuel solution: W%: ^{235}U: 2.629, ^{238}U: 10.683, O: 76.456, H: 8.659, N: 1.564	1.63	g/cm^3
Stainless Steel cover plate: W%: Fe: 69.5, Cr: 19, Ni: 9.5, Mn: 2.0	6.50	g/cm^3
D_2O reflector: W%: D: 33.33, O: 66.67	1.105	g/cm^3
Core dimension	36 × 41	cm

can be used. However, if the pH is too low, the ion exchange resin, which is used for ^{99}Mo recovery from the aqueous solution, is less effective [3].

The used nitrate solution contains 170 g/L of enriched U. A lower uranium salt concentration in the fuel solution results in a larger distribution coefficient (K_d) for Mo(VI), and therefore a more effective and efficient recovery of ^{99}Mo from such solutions [1]. Uranyl nitrate solubility in water is 660 g/L [8].

The effective multiplication factor of the modeled core was adjusted to < 0.93. The CYCLONE30 proton accelerator with a maximum beam current of 150 μA and energy of 30 MeV was used to induce the fission process inside the ADHR.

Light water coils of 3 cm diameter were used to cool the aqueous solution. The cross-sectional view of the core modeled by MCNPX code is depicted in Fig. 1.

Uranium nitrate solution was used as fuel of the modeled AHR. ^{99}Mo, ^{89}Sr, and ^{131}I production efficiency and the safety factors of the nuclear reactor were investigated. Accelerated proton particles were used to induce fission in the ADHR. The energy range from 10 to 30 MeV was investigated. Four different beam windows—^{232}Th, 20% enriched U, tungsten, and stainless steel—were investigated to obtain the maximum fission power in the aqueous fuel. The best beam window was chosen so that it could bear the deposited heat and deliver an optimized neutron spectrum to the fuel solution. The radial and axial neutron flux distributions inside the aqueous solution were calculated using the mesh tally card of the computational code. The radial and axial deposited power distributions were calculated using the mesh tally card. The reactivity coefficients of fuel, coolant, and moderator were calculated using the Temperature (TMP) card and temperature-related cross section library of 0.71c from endf70 in the MCNPX. The void reactivity effects of the coolant, reflector, and the solution fuel were calculated. The delayed neutron fraction and effective delayed neutron fraction were calculated for the modeled ADHR. The burnup calculation of the fuel solution was performed at a calculated deposited fission power by proton beam current. The burnup calculations were carried out for 1 week using the BURN card available in the used code. The production rate of ^{99}Mo, ^{89}Sr, and ^{131}I after the burnup time was investigated. The production rate of long half-life alpha emitter radioisotopes after the burnup time was investigated. The modeled ADHR radioisotope production rate was compared with the available theoretical and experimental data. Purification of molybdenum, iodine, xenon, and strontium from the other fission products was discussed.

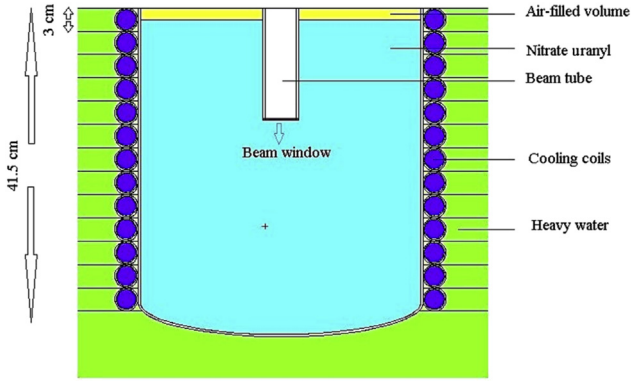

Fig. 1 – Cross-sectional view of the modeled core.

3. Result and discussion

When accelerated proton particles pass through the used beam window, (p,nx), (p,fiss), (p,n), (p,2n), and the other reactions can produce some neutrons inside the window. The produced neutrons initiate the fission process over the subcritical aqueous reactor. SS-304, 20% enriched U, ^{232}Th, and tungsten beam windows were used separately, and the deposited power from the fission process was calculated inside the ADHR. The results showed that, for a 2-mm beam window exposed to 10 MeV, there was not much difference in power caused by the different beam window materials. The calculations showed that the proton energy enhancement could increase the produced power noticeably, especially in the case of the ADHR equipped with fissionable beam windows (Fig. 2).

As Fig. 2 illustrates, the application of a 2-mm ^{232}Th beam window irradiated by 30 MeV protons can produce ~5.1 kW power inside the ADHR. This is 1.81 times the power produced by a tungsten window and 2.47 times the power produced by a stainless steel one. The deposited power inside the ADHR that uses a 20%-enriched U window is 1.20 times that of the ^{232}Th beam window. Hence, a fissionable beam window could increase the extracted fission power up to 80% or even higher in comparison with a nonfissionable beam window. Obviously, the fissionable windows can remarkably increase the produced power inside the modeled ADHR reactor. Considering the available experimental cross section data in the EXFOR library, it is well understood that the proton-induced fission cross section of $^{235/238}$U changes noticeably between 10 and 30 MeV, and the reaction cross section is more than 1,000 mb at 20 MeV (Fig. 3A).

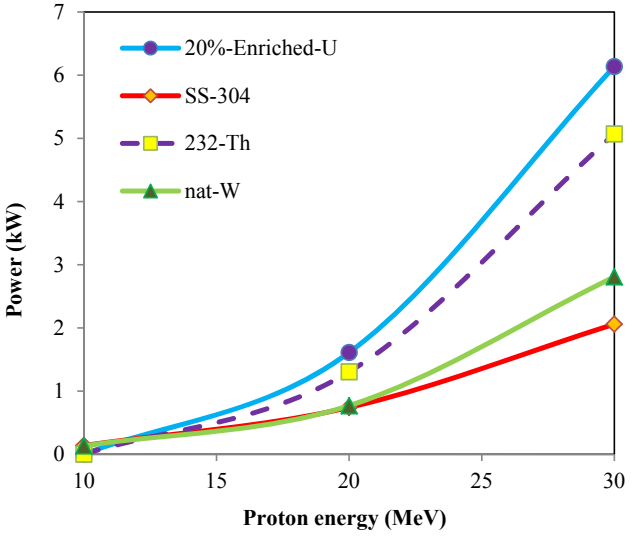

Fig. 2 – Dependence of the produced power inside the aqueous reactor on beam window type and projectile particle energy. Window thickness, 2 mm; proton current, 150 μA.

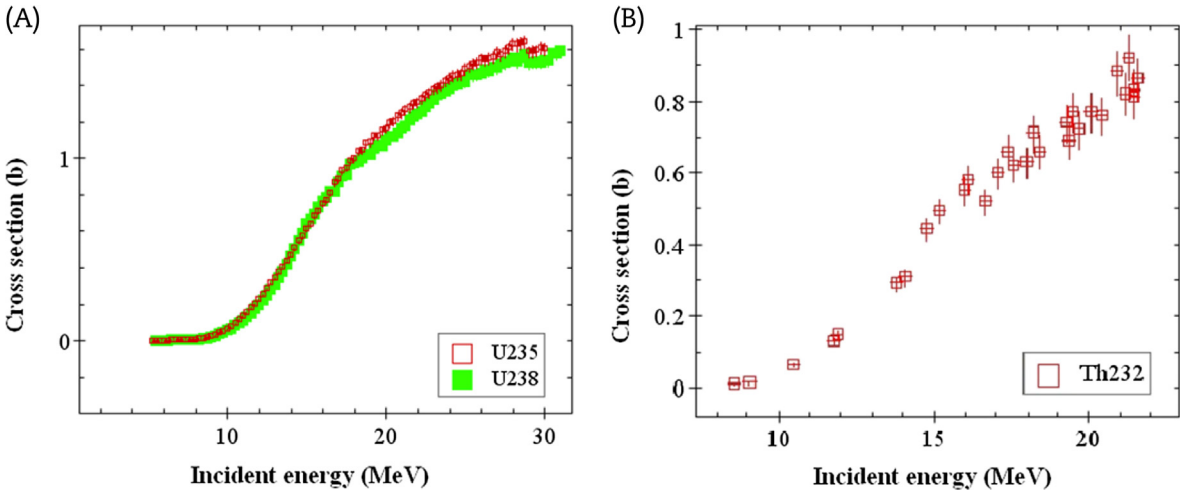

Fig. 3 – Variations of proton-induced fission cross section of ^{235}U and ^{238}U and ^{232}Th on proton energy [10–12]. (A) ^{235}U and ^{238}U. (B) ^{232}Th.

Also, the proton-induced fission cross section of ^{232}Th increases considerably between 10 and 30 MeV. The reaction cross section is more than 750 mb at 20 MeV (Fig. 3B).

The effect of the beam window thickness on the produced power was investigated using 30-MeV protons irradiating the beam windows of different materials separately. The calculations showed that increasing the thickness of the enriched uranium window from 0.5 mm to 2 mm did not increase the extracted power from the aqueous solution reactor (<3%). By increasing the ^{232}Th window thickness from 0.5 mm to 1 mm, about 26% power enhancement was obtained, whereas more enhancement of the window thickness would not result in an outstanding improvement in the produced power (<3%). For the tungsten beam window, different thicknesses (0.5–2 mm) did not significantly affect the extracted power of the ADHR. The SS-304 beam window thickness enhancement from 0.5 to 1.5 mm increased the produced power inside the aqueous reactor significantly (~50%) whereas more thickness enhancement did not increase the produced power more than 1.5% (Fig. 4). This phenomenon can be related to (p,2n) and (p,3n) efficiency enhancement by increasing the window thickness [13].

It seems that the fissionable windows could be considered as favorable candidates for increasing the extracted power from the ADHR. Hence, the deposited heat inside the fissionable beam windows was calculated to determine the window temperature profile during irradiation. A static situation was proposed for the calculation, no heat removal was imagined for the investigated window, and the fluid fuel impact on the heat variability of the beam window was not involved. The calculations showed that the ^{232}Th window with 2-mm thickness experiences a maximum temperature rise of ~1,500°C during the window irradiation by 30 MeV protons with 150 μA current. However, the 20% enriched U window experiences a maximum temperature rise of ~4,500°C under the same conditions (Fig. 5).

The obtained results show that the investigated enriched uranium could not be considered a worthy material for the beam window because of its low melting point (1,135°C) and poor thermal conductivity (27 W/mK). Therefore, ^{232}Th seems to be a favorable option because of its higher melting point (1,750°C) and thermal conductivity (54 W/mK) [14]. Consequently, a 2-mm ^{232}Th window was chosen for further calculations, and 30 MeV proton energy was proposed for the calculations.

The radial distribution of thermal, epithermal, and fast neutrons in the subcritical reactor showed that the most prominent neutron population over the subcritical core belongs to thermal neutrons. A neutron flux in the order of 10^{10} n/s cm^2 is available inside the subcritical core (Fig. 6).

The neutron spectra determination inside the aqueous reactor and the heavy water reflector showed that about 40%

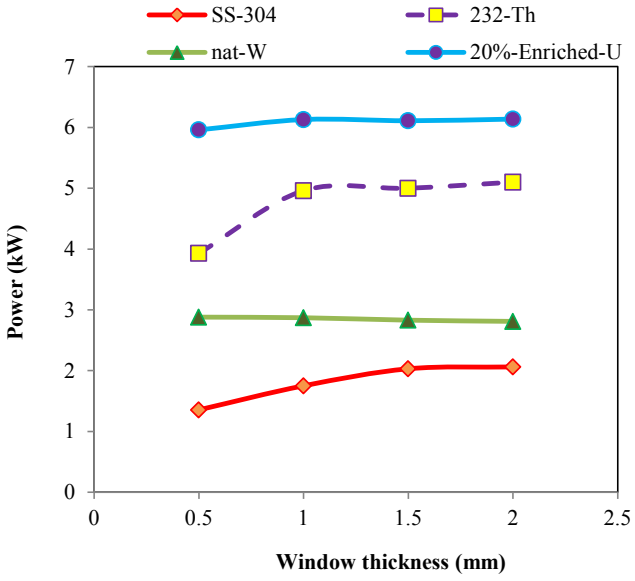

Fig. 4 – Dependence of the produced power inside the aqueous reactor on beam window thickness. Proton current, 150 μA; proton energy, 30 MeV.

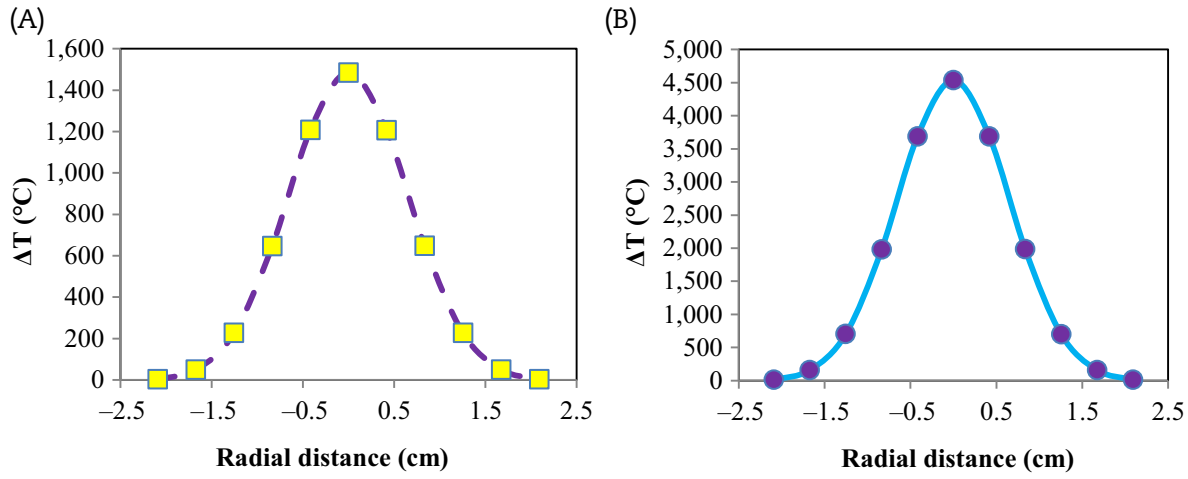

Fig. 5 – Radial variations of the 2-mm beam window temperature. Proton current, 150 μA; proton energy, 30 MeV. (A) ^{232}Th. (B) 20% enriched U.

of the neutrons inside the reactor core are thermal and about 19% of them are epithermal. In the heavy water reflector, about 68% of the neutrons are thermal and about 18% are epithermal (Fig. 7).

Void formation is an unavoidable concern in aqueous reactors. The calculations showed that the fuel void reactivity is strongly negative [~−6 mk/(void%) on average], the reflector void reactivity is a little negative [~−0.3 mk/(void%) on average], and the coolant void reactivity is slightly positive [~+0.05 mk/(void%) on average]. The highly negative total void reactivity ensures the exceptional safety of the subcritical core (Fig. 8).

The calculations for the neutronic parameters show that the effective multiplication of the modeled subcritical core is 0.93155 ± 20 pcm. The subcritical core β and β_{eff} parameters were 753 and 651 pcm, respectively. The fuel, coolant, and reflector temperature reactivity coefficients were −2.05, +0.81, and −0.84 pcm/°C, respectively. The fission per nonfission absorption ratio of the aqueous reactor driven by 30 MeV protons with 150 μA current is 1.31, and the fission per absorption ratio is 0.58.

The radial and axial power depositions resulting from the fission process are shown in Figs. 9A and 9B, respectively. According to the results in the radial direction, the maximum heat deposition is experienced by the solution around the beam tube. In the axial direction, the maximum heat deposition is experienced by the central section of the aqueous solution. The beam line pathway is clearly observable in Fig. 9B, which creates an asymmetry in axial power distribution. However, the fluid fuel circulation of the subcritical reactor eliminates concerns with unsmooth burnups of the loaded fuel so that axial and radial power peak factors are less important in the case of such reactors.

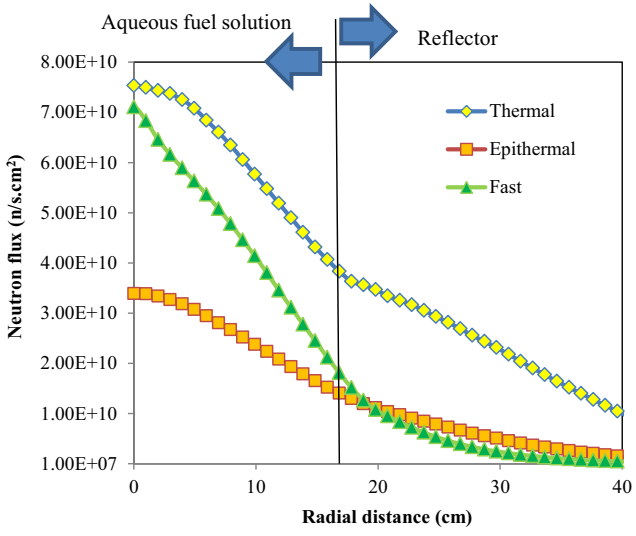

Fig. 6 – Radial distribution of neutron flux. ^{232}Th beam window thickness, 2 mm; proton current, 150 μA; proton energy, 30 MeV.

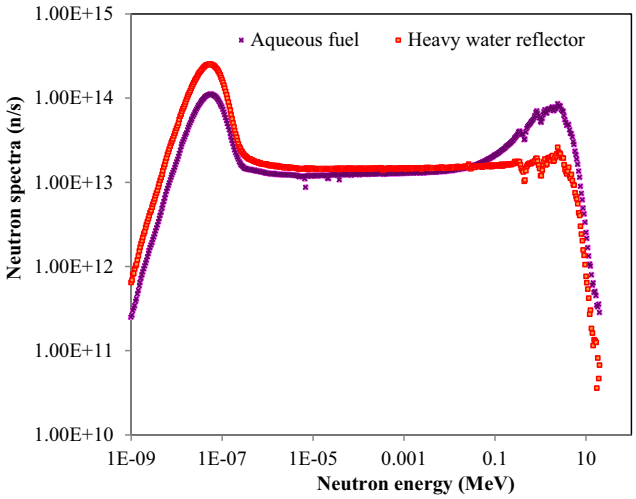

Fig. 7 – Dependence of neutron current inside the aqueous fuel and reflector on energy.

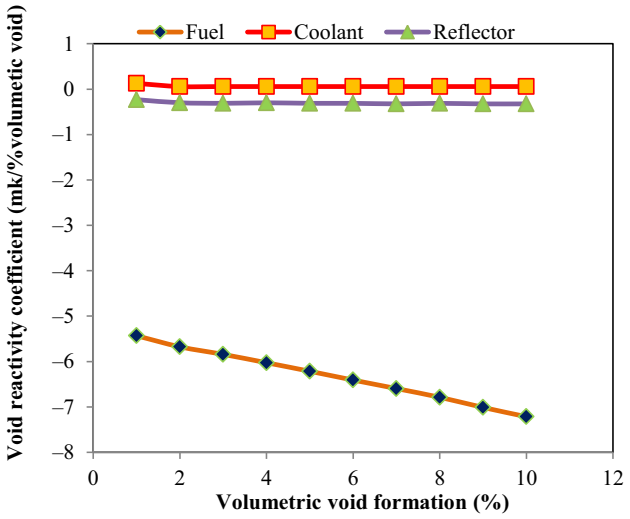

Fig. 8 – Dependence of void reactivity coefficient on volumetric void formation percentage.

The radial and axial integrated neutron flux distributions are shown in Figs. 10A and 10B, respectively. In the radial direction, the neutron flux peak is located at the center of the aqueous reactor, whereas in the axial direction the neutron flux peak is located near the beam window.

Burnup calculations were carried out for the ADHR exposed to 5.10 kW power using 30 MeV protons, which bombard the ^{232}Th beam window with a current of 150 μA. To compare the efficiency of ^{232}Th and 20% enriched U beam windows for production of the proposed radioisotopes, the burnup calculation was repeated for the ADHR at 6.14-kW power delivered to the subcritical reactor via proton irradiation of the enriched uranium beam window.

The results show that the ^{99}Mo radioisotope is produced as carrier-free in the burnt aqueous solution. Its production yield using 6.14 kW power is about 20% more than that obtained at 5.10 kW power induced by the ^{232}Th beam window bombardment. ^{89}Sr will not be produced as carrier-free; the ^{89}Sr/^{90}Sr ratio in the investigated burnt fuel is about 159 at end of cycle (EOC) (Table 2).

For medical uses, the fraction of ^{90}Sr activity should not exceed 0.0002% [15], but there is about 0.62% accompaniment of ^{90}Sr (half-life = 28.79 years) in the aqueous burnt solution at EOC.

As shown in Table 2, about 368 Ci of ^{131}I is produced in the burnt aqueous solution. ^{129}I (half-life = 157 × 10^7 years, activity at EOC = 1.06 × 10^{-7} Ci), ^{132}I (half-life = 2.295 hours, activity at EOC: 965.2 Ci), ^{133}I (half-life = 20.8 hours, activity at EOC = 1943 Ci), ^{134}I (half-life = 52.5 minutes, activity at EOC = 2,280 Ci), and ^{135}I (half-life = 6.57 hours, activity at EOC = 182.9 Ci) are produced at EOC, too. Whereas the ^{129}I activity is ignorable, ^{131}I carrier-free product could be obtained after a proposed time, which is intended to allow the other radioisotopes to decay to stable Xe and Cs isotopes. As shown in Fig. 11, after 8 days decay time the ^{131}I activity will be 184.35 Ci, the ^{133}I activity will be 3.2 Ci, and the ^{135}I activity will be 3 μCi. According to the calculations, after 20 days the ^{131}I activity will be 65.36 Ci and the ^{133}I activity will be 200 μCi. After the proposed time, the concentration of the other iodine isotopes is approximately zero.

Our calculations show that $^{131-136}$Xe isotopes are produced inside the irradiated aqueous solution, and except for ^{133}Xe and ^{135}Xe the others are stable. After 216 hours decay of the collected xenon gas, 62.6 Ci of ^{133}Xe and 0.0001 Ci of ^{135}Xe will remain, which gives a ^{135}Xe/^{133}Xe activity ratio of less than 1 × 10^{-6} or 0.0001% (Fig. 12). Noncarrier added product or a product with low concentrations of impurities is acceptable for radiomedicine aims [16].

According to Table 3, many radioisotopes are produced in the ADHR. As the burnup data show, these fission products have high concentrations, which complicates the separation and purification of ^{99}Mo or other proposed radioisotopes from the aqueous solution in comparison with the ^{98}Mo(n,γ) production method.

The ARGUS reactor uses 73.2 g/L of 90% enriched ^{235}U in UO_2SO_4 water solution to produce ^{89}Sr and ^{99}Mo radioisotopes [16]. Another method used in the ARGUS aqueous solution reactor relies on ^{89}Kr discharge from the burnt solution in 20-

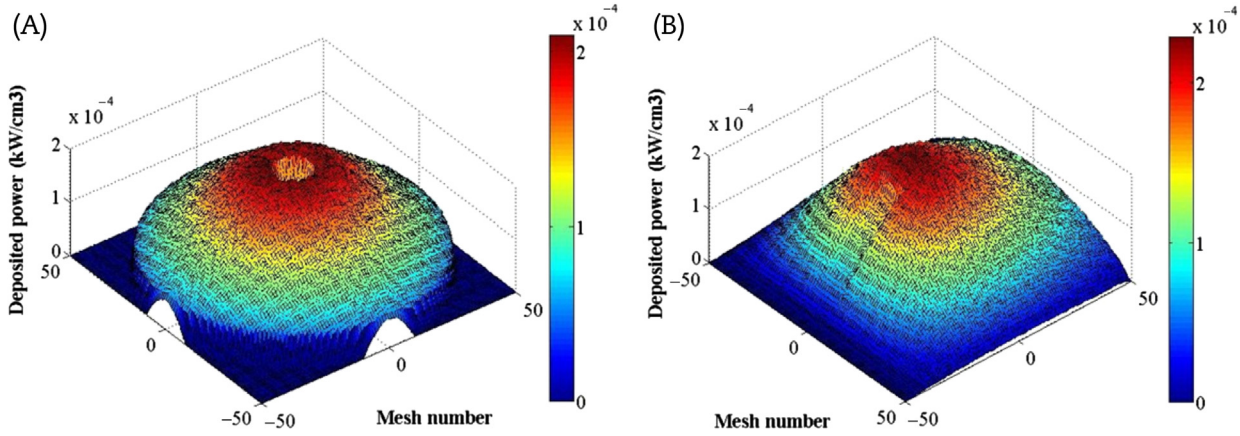

Fig. 9 – Distribution of deposited heat. (A) Radial. (B) Axial. ^{232}Th beam window thickness, 2 mm; proton current, 150 μA; proton energy, 30 MeV.

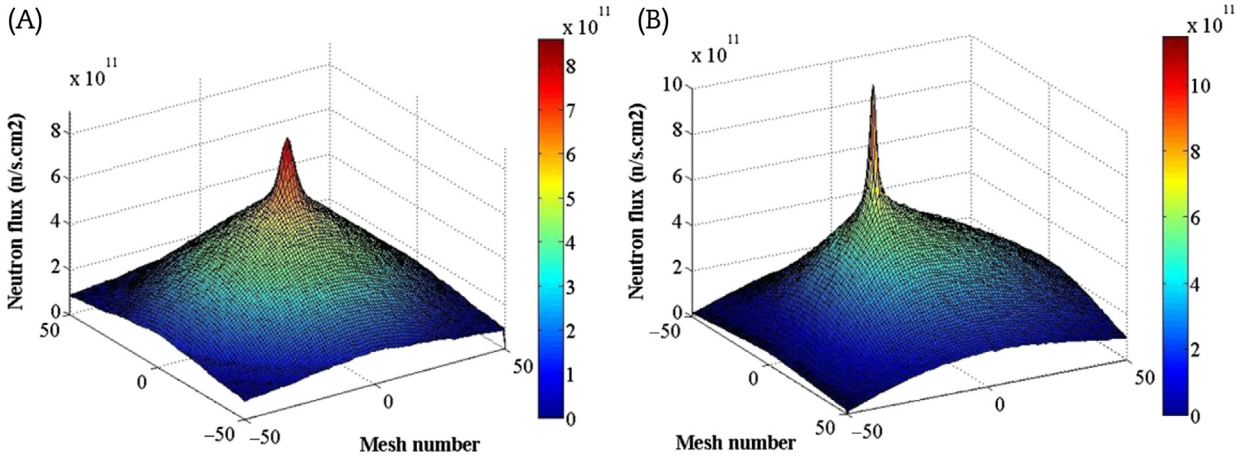

Fig. 10 – Integrated neutron flux distribution. (A) Radial. (B) Axial. ^{232}Th beam window thickness, 2 mm; proton current, 150 μA; proton energy, 30 MeV.

minute time steps, which concludes in 1.216 mCi/g/kW carrier-free production of ^{89}Sr [15].

^{89}Kr production occurred in the aqueous modeled core, but the code used cannot calculate its production yield because the CINDER90 code only solves the decay chain equations up to ^{86}Kr [17].

To sum up, a comparison between the other methods and the modeled ADHR can reveal the potential of such systems for production of radioisotopes.

The ^{89}Y(n, p)^{89}Sr reaction yields 0.01 Ci/g-Y using the target irradiation in a 60-MW BOR-60 nuclear reactor for 30 days [18]. The corresponding value in this work is ~0.104 Ci/g ^{235}U using the ADHR at 5.10 kW power for 7 days, which is not a carrier-free product.

The saturation yield of ^{99}Mo via ^{235}U irradiated in a thermal neutron flux of 2×10^{14} n/s cm^2 is about 335 Ci/g [19]. The usage of ^{98}Mo for ^{99}Mo production is currently only done in small-scale facilities. Because of the low specific activity of ^{99}Mo produced by this process (~1 Ci/g ^{98}Mo), as well as the lower cross section for ^{99}Mo production compared to fission, this technique is not suited for large-scale production [20].

Another technique is a neutron-capture scheme involving the irradiation of metallic ^{98}Mo or molybdenum trioxide Mo_2O_3 (natural or enriched in ^{98}Mo) with thermal neutrons in a nuclear reactor. Since both the target material and final product are chemically identical species, these components cannot be separated. The final ^{99}Mo is of low specific activity (<10 Ci/g Mo) and consists of a large quantity of bulk chemical molybdenum [21].

The corresponding value in this work is ~1.25 Ci/g ^{235}U after 7 days of burnup, which is a carrier-free product.

Similar accelerator driven reactor projects are being performed for ^{99}Mo production such as SHINE (Subcritical Hybrid Intense Neutron Emitter). In this system, deuteron gas flows into an ion source and is ionized by microwaves; an accelerator pushes the ions toward a target chamber (300 keV); the accelerated deuterons strike tritium gas in the target, creating neutrons at 2×10^9 n/s/W. This system has several advantages: it involves mature accelerator technology; it is inherently safe; it uses LEU (19.75%); it reduces nuclear waste; and the aqueous target simplifies chemical extraction. An industrial-scale prototype is now under development, with an anticipated production of >500 6-day Ci/wk [22]. Our obtained data show that the modeled system has good potential for ^{99}Mo production (~325 6-day Ci/wk) and satisfactorily competes with the SHINE facility.

ADONIS is another project that was planned to produce ^{99}Mo by proton irradiation of solid LEU targets. ADONIS relies on a high-energy high-current cyclotron coupled to a subcritical assembly. The proton beam impinges on a conical spallation target made of tantalum to generate a high-intensity neutron flux. The Ta target is surrounded by four cylindrical layers of HEU targets interleaved with beryllium moderation rings. Overall, 1,470 6-day Ci/wk and 4,940 6-day Ci/wk of ^{99}Mo were obtained with this procedure using protons of 200 and 350 MeV with a constant beam current of 1 mA induced on a 5-cm-thick target separately [7].

Table 2 – Activity of some produced radioisotopes after 7 days irradiation of aqueous solution using 30 MeV protons of 150 μA current.

	^{99}Mo $_{6\text{-d Ci}}$	^{99}Mo$_{EOC}$ (Ci)	^{131}I$_{EOC}$ (Ci)	^{89}Sr$_{EOC}$ (Ci)	^{90}Sr$_{EOC}$ (Ci)	k_{eff} at BOC	k_{eff} at EOC
20% Enriched U beam window	389.5	1,769	441.6	150.9	0.95	0.92977	0.92494
^{232}Th beam window	324.7	1,475	368.2	125.8	0.79	0.92977	0.92575
Half-life	–	65.94 hr	8.02 d	50.53 d	28.79 yr	–	–

BOC, beginning of cycle; EOC, end of cycle.

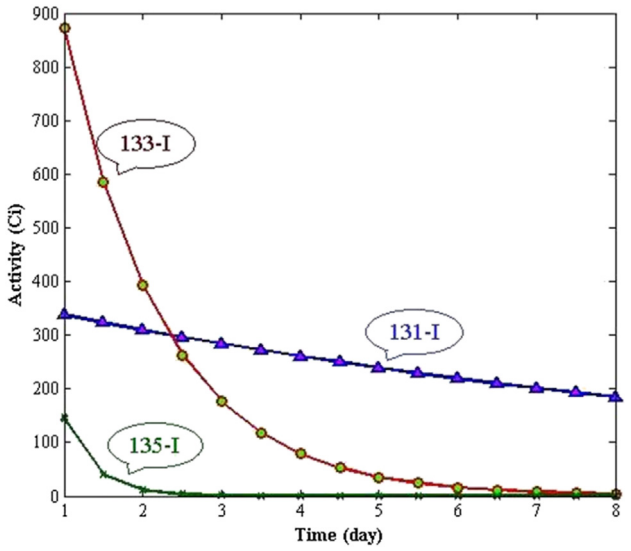

Fig. 11 – Comparison of ^{131}I, ^{133}I, and ^{135}I radioisotopes' decay on time.

Depending on the kW/L deposited power inside a modeled AHR, different produced concentrations of ^{99}Mo (584–2,514, 6-day Ci/wk correspond to 0.33–1.43 kW/L) were reported for a nitrate solution containing 20% enriched uranium [23]. In our modeled ADHR, the deposited power is 0.127 kW/L, and a ^{99}Mo production rate of ~325 6-day Ci/wk was obtained. A ^{99}Mo production rate of ~180 6-day Ci/wk was reported for natural uranium irradiation by 50 MeV electrons; the accelerated charged particles induce a gamma-fission reaction in the solid target [24]. Other accelerator-based proton-fission induced methods reported about 6,000 6-day Ci/wk production of ^{99}Mo via 1 GeV proton irradiation of an LEU target [25]. The Argentine 5-MW RA-3 research reactor uses LEU solid targets to produce 200 6-day Ci/wk of ^{99}Mo [26].

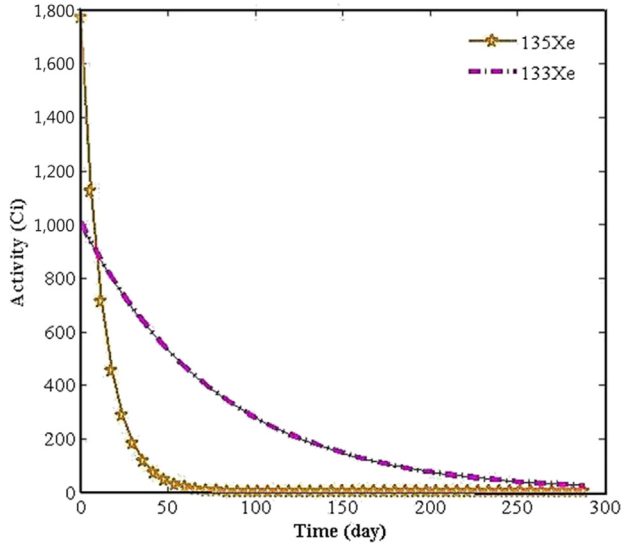

Fig. 12 – Comparison of ^{133}Xe and ^{135}Xe radioisotopes' decay on time.

Table 3 – Activity of some produced radioisotopes with values of >1 mCi after burnup of the aqueous solution using 30 MeV protons of 150 μA current.

Radioisotopes	EOC	6-d Ci	Half-life (d)
Nonactinide			
^{133}Xe	1,010	158.2	5.243
^{135}Xe	1,770	0.032	0.380
^{103}Ru	102.6	92.64	39.260
^{106}Ru	1.52	1.480	373.59
^{140}Ba	572.5	412.9	12.725
^{91}Y	123.8	115.3	58.51
^{97}Nb	1,756	0.0	0.050
^{95}Zr	138.1	129.4	64.02
^{105}Rh	268.7	15.98	1.473
^{132}Te	968.7	264.5	3.204
^{140}La	401.7	33.71	1.6781
^{141}Ce	228.2	200.7	32.501
^{143}Ce	1,683	81.98	1.376
^{144}Ce	27.04	26.71	284.893
^{145}Pr	1,145	6×10^{-5}	0.2493
^{147}Nd	233.3	159.7	10.98
^{151}Sm	0.013	0.012	2,160
^{147}Pm	0.631	0.628	957.541
^{149}Pm	278.7	42.50	2.211
^{151}Pm	119.9	0.018	0.4733
Actinide			
^{239}NP	7,813	1,338	2.3565
^{239}Pu	0.005	0.005	88.0015×10^{5}
^{236}U	3×10^{-6}	3×10^{-6}	854.830×10^{7}

EOC, end of cycle.

In addition, 770–1,100 6-day Ci of ^{99}Mo production using AHRs has been reported [27].

Routine chemical reprocessing, which is used by different ^{99}Mo production centers, could be used in the ADHR facility to recover Xe, Mo, Sr radioisotope, and I.

Released ^{133}Xe, other isotopes of noble gases, and isotopes of iodine (e.g., ^{131}I, ^{132}I, and ^{133}I) are trapped by means of absorption and adsorption techniques and filling of pre-evacuated tanks. The released iodine is trapped on platinum asbestos and then purified. Radioxenon is released from the aqueous solution, trapped on copper clippings, and then purified [28].

A TiO_2 (80 μm) column could be used for the recovery of Mo from uranyl nitrate solutions containing 450 g U/L and 1M HNO_3. Countercurrent stripping using 0.1M NaOH can achieve full recovery of Mo [29].

^{89}Sr was separated from irradiated uranium by absorption on a column of polyantimonic acid using 4M HNO_3 medium. ^{89}Sr can be recovered by elution with 1M $AgNO_3$ and 8M HNO_3 at 75°C [30].

Thus, a suitable reprocessing diagram should be planned for these aqueous reactors to obtain the highest yield of the recovered radioisotopes without changing the nature of the uranyl nitrate solution much.

Aqueous homogenous subcritical reactors have good potential to produce the required radioisotopes using accelerator-driven operation of the reactor. High negative reactivity coefficients, less need for modification of the loaded fuel in short time steps, as well as electronic control of the aqueous reactor by an accelerator—in contrast to the

customary AHRs such as ARGUS—are admirable advantages of aqueous subcritical accelerator-driven reactors. The good potential for ^{99}Mo carrier-free production (~1,500 Ci/wk at EOC) using LEU fuel and a low-energy proton accelerator can reveal more economic alternatives for production of ^{99}Mo that do not depend on large-scale research nuclear reactors. The aqueous reactor has potential for other radioisotopes such as ^{131}I, ^{133}Xe, and ^{89}Sr.

Conflicts of interest

All contributing authors declare no conflicts of interest.

REFERENCES

[1] M.E. Bunker, Early Reactors, from Fermi's Water Boiler to Novel Power Prototypes, Los Alamos Science, New Mexico, United States, 1983, pp. 124–131.

[2] J.A. Lane, H.O. Macpherson, F. Maslan, Fluid Fuel Reactors, Addison-Wesley Publishing, (MA), Geneva, Switzerland, 1958, p. 345.

[3] A. Pablo, Y.D. Baranaev, A.M.M.L. Barbosa, F. Barbry, E. Bradley, I. Goldman, G.W. Neeley, et al., IAEA-TECDOC-1601. Homogeneous Aqueous Solution Nuclear Reactors for the Production of Mo-99 and Other Short Lived Radioistotopes, Nuclear Fuel Cycle and Materials Section International Atomic Energy Agency, Vienna, Austria, 2008.

[4] F. Stichelbaut, Design of New Solutions to Produce 99Mo Using Sub-critical Systems IBA, Belgium, Science and Technology Facilities Council, U.K., 2011.

[5] S. Chemerisov, A.J. Youker, A. Hebden, N. Smith, P. Tkac, C.D. Jonah, J. Bailey, V. Makarashvili, B. Micklich, M. Kalensky, G.F. Vandegrif, Development of the Mini-SHINE/MIPS Experiments, Molybdenum-99 Topical Meeting, New Mexico, Argonne National Laboratory, Dec. 4–7, 2011.

[6] F. Stichebaut, Y. Jongen, Design of accelerator-based solutions to produce 99Mo using lowly-enriched uranium, Prog. Nucl. Sci. Technol. 2 (2011) 284–288.

[7] N.R. Stevenson, M.K. Korenko, R.E. Schenter, F-M. Su, Hybrid Accelerator-Heavy Water System for Production of a Reliable, Domestic Supply of Molybdenum-99 without the Use of Highly Enriched Uranium, Advanced Medical Isotope Corp, Kennewick (WA), USA.

[8] K. Elgin, A Study of the Feasibility of ^{99}Mo Production inside the TU Delft Hoger Onderwijs Reactor, Thesis, October 2014.

[9] M.L. Fensin, Development of the MCNPX Depletion Capability: A Monte Carlo Depletion Method that Automates the Coupling Between MCNPX and CINDER90 for High Fidelity Burnup Calculations, Florida University, 2008.

[10] J.R. Boyce, Proton-induced Fission Cross Sections of the Uranium Isotopes ^{233}U, ^{234}U, ^{235}U, ^{236}U, and ^{238}U, PhD thesis, Duke University, Durham, North Carolina, United States, 1972.

[11] J.R. Boyce, D. Hayward, R. Bass, H.W. Newson, E.G. Bilpuch, F.O. Purser, H.W. Schmitt, Absolute cross sections for proton-induced fission of the uranium isotopes, Phys. Rev. C-10 (1974) 231–244.

[12] G.H. McCormick, B.L. Cohen, Fission and total reaction cross sections for 22-Mev protons on ^{232}Th, ^{235}U, and ^{238}U, Phys. Rev. 96 (1954) 722–724.

[13] EXFOR—IAEA Nuclear Data Services. Available from: https://www-nds.iaea.org/exfor/ (cited Oct 6, 2015).

[14] Thermal Conductivity for all the elements. Available from: periodictable.com/Properties/A/ThermalConductivity.html (cited 13 Nov 2015).

[15] A. Isnaeni, M.S. Aljohani, T.G. Aboalfaraj, S.I. Bhuiyan, Analysis of ^{99}Mo production capacity in uranyl nitrate aqueous homogeneous reactor using ORIGEN and MCNP, Atom Indones. J. 40 (2014) 40–43.

[16] D.Y. Chuvilin, J.D. Meister, S.S. Abalin, R.M. Ball, G.Y. Grigoriev, V.E. Khvostionov, D.V. Markovskij, H.W. Nordyke, V.A. Pavshook, An interleaved approach to production of ^{99}Mo and ^{89}Sr medical radioisotopes, J. Radioanal. Nucl. Chem. 257 (2003) 59–63.

[17] D.B. Pelowitz, Users' Manual Version of MCNPX2.6.0, LANL, LA-CP-07-1473, Los Alamos National Laboratory, New Mexico, United States, 2008.

[18] D. Saha, J. Vithya, G.V.S. Ashok Kumar, K. Swaminathan, R. Kumar, C.R. Venkata Subramani, P.R. Vasudeva Rao, Feasibility studies for production of ^{89}Sr in the Fast Breeder Test Reactor (FBTR), Radiochim. Acta 101 (2013) 667–673.

[19] Y. Jongen, P. Cohilis, P. Dhondt, L. Van Den Durpel, H. Aït Abderrahim, A Proton-driven, intense, subcritical, fission neutron source, in: Proceedings of the 14th International Conference on Cyclotrons and Their Applications, Cape Town (South Africa), 1995, pp. 610–613.

[20] K. Bertsche, Accelerator Production Options for ^{99}Mo, Proceedings of IPAC'10 08 Applications of Accelerators, Technology Transfer and Industrial Relations, U01 Medical Applications, (MOPEA025), Kyoto (Japan), May, 2010, pp. 121–123.

[21] M. Khan, T. Jabbar, M. Asif, M.I. Anjum, M. Dilband, K. Khan, A. Jabbar, W. Arshed, Radiostrontium separation from sodium molybdate solution and its measurement using LSA: an application to radiopharmaceutical analysis, J. Radioanal. Nucl. Chem. 299 (2014) 577–582.

[22] WOSMIP III—Workshop on Signatures of Medical and Industrial Isotope Production, Castello di Strassoldo di Sopra, Strassoldo, Friuli-Venezia Giulia, Italy, Prepared for the U.S. Department of Energy under Contract DE-AC05-76RL01830, 19–22 Jun, 2012.

[23] S. K. Klein, ^{99}Mo Production Technology Development at LANL, LA-UR 11-05325, Los Alamos National Laboratory, New Mexico, United States.

[24] A. Fong, T.I. Meyer, K. Zala, Making Medical Isotopes: Report of the Task Force on Alternatives for Medical-isotope Production, TRIUMF, Vancouver (Canada), 2008.

[25] S. Buono, N. Burgio, L. Maciocco, Technical Evaluation of an Accelerator-driven Production of Mo-99 for Tc-99m Generators at CERN (MolyPAN Project), 2010 https://indico.cern.ch/event/70767/.../Maciocco_Mo99_talk.pdf, Geneva, Switzerland.

[26] Available from: Production and Supply of Molybdenum-99, International Atomic Energy Agency, Vienna, Austria, 2010 https://www.iaea.org/.../gc54inf-3-a (cited Oct 6, 2015).

[27] M.V. Huisman, Medical Isotope Production Reactor, Reactor Design for a Small Sized Aqueous Homogeneous Reactor for Producing Molybdenum-99 for Regional Demand, Master thesis, Delft University, Delft, Netherlands, 2013, p. 11.

[28] IAEA-TECDOC-1051, Management of Radioactive Waste from ^{99}Mo Production, 1998.

[29] D.C. Stepinski, E.O. Krahn, P.-L. Chung, G.F. Vandegrift, Design of Column Separation Processes for Recovery of Molybdenum from Dissolved High Density LEU Target, Argonne National Laboratory, New Mexico, United States, 2011.

[30] R.N. Varma, K.L.N. Rao, G.N. Chavan, K.R. Balasubramanian, T.S Murthy, Separation of ^{89}Sr from Irradiated Uranium Using Polyantimonic Acid, 1982, 4 pp, Department of Atomic Energy, Bombay (India), 7–11 Dec 1982. Radiochemistry and Radiation Chemistry Symposium, Pune (India).